Developmental Cell
Article

Chromatin Regulation by BAF170 Controls Cerebral Cortical Size and Thickness

Tran Cong Tuoc,[1,4,5] Susann Boretius,[2,4,6] Stephen N. Sansom,[3,7] Mara-Elena Pitulescu,[1,8] Jens Frahm,[2,4] Frederick J. Livesey,[3] and Anastassia Stoykova[1,4,*]
[1]Research Group of Molecular Developmental Neurobiology, Department of Molecular Cell Biology
[2]Biomedizinische NMR Forschungs GmbH
Max-Planck-Institute for Biophysical Chemistry, 37077 Göttingen, Germany
[3]Gurdon Institute and Department of Biochemistry, University of Cambridge, Cambridge CB2 1QN, UK
[4]Center for Nanoscale Microscopy and Molecular Physiology of the Brain (CNMPB), 37075 Göttingen, Germany
[5]Current address: Department of Neuroanatomy, Universitätsmedizin Göttingen, 37075 Göttingen, Germany
[6]Current address: Klinik für Diagnostische Radiologie, Universitätsklinikum Schleswig-Holstein, 24105 Kiel, Germany
[7]Current address: MRC Functional Genomics Unit, University of Oxford, Oxford OX1 3PT, UK
[8]Current address: Max-Planck-Institute for Molecular Biomedicine, Münster 48149, Germany
*Correspondence: astoyko@gwdg.de
http://dx.doi.org/10.1016/j.devcel.2013.04.005

SUMMARY

Increased cortical size is essential to the enhanced intellectual capacity of primates during mammalian evolution. The mechanisms that control cortical size are largely unknown. Here, we show that mammalian BAF170, a subunit of the chromatin remodeling complex mSWI/SNF, is an intrinsic factor that controls cortical size. We find that conditional deletion of *BAF170* promotes indirect neurogenesis by increasing the pool of intermediate progenitors (IPs) and results in an enlarged cortex, whereas cortex-specific *BAF170* overexpression results in the opposite phenotype. Mechanistically, BAF170 competes with BAF155 subunit in the BAF complex, affecting euchromatin structure and thereby modulating the binding efficiency of the Pax6/REST-corepressor complex to Pax6 target genes that regulate the generation of IPs and late cortical progenitors. Our findings reveal a molecular mechanism mediated by the mSWI/SNF chromatin-remodeling complex that controls cortical architecture.

INTRODUCTION

The mammalian neocortex is constructed from multiple neuronal and glial subtypes that are organized radially in six layers and tangentially in several functional domains. Layer-specific excitatory glutamatergic projection neurons are produced in a specific temporal order by radial glial cells (RGCs) through two modes of neurogenesis, direct and indirect (Götz and Huttner, 2005; Kriegstein et al., 2006). In direct neurogenesis, an RGC located at the apical surface of the ventricular zone (VZ) divides asymmetrically to produce a new RGC and a neuron. Neurons generated during early neurogenesis (E10.5–E14.5 in mouse) are located predominantly in the lower or deep cortical layers (LL, L6, L5). In indirect neurogenesis, the RGC also self-renews, but instead of producing a neuron, it generates an intermediate progenitor (IP) that migrates into the subventricular zone (SVZ), where it undergoes a limited number of (1–3) symmetric divisions, amplifying the acquired neuronal fate at each specific developmental stage. Although IPs are present in the germinal zones as early as E10.5 they contribute more significantly to generation of neurons with upper layer identities (UL, L4–L2) during late neurogenesis (Pontious et al., 2008).

Work from our group and others indicates that the transcription factor (TF) Pax6 is an intrinsic determinant of RGCs, promoting the indirect mode of cortical neurogenesis, involved predominantly in the generation of neurons with upper layer identities (Georgala et al., 2011; Götz et al., 1998; Quinn et al., 2007; Sansom et al., 2009; Tuoc et al., 2009). Acquisition of distinct neuronal fates from multipotent stem cells and progenitors depends on activation and/or repression of distinct transcriptional programs, a process in which control over epigenetic chromatin remodeling through the ATP-dependent multisubunit mSWI/SNF complexes (also known as BAF complexes) plays a decisive role (Yoo and Crabtree, 2009). As recently shown, the transition from proliferating embryonic stem cells (with an esBAF complex) toward committed neuronal precursors (with a neural progenitor-specific complex, npBAF) is accompanied by initiation of transcription of the BAF170 subunit, which replaces one of the two BAF155 subunits in the esBAF (Ho et al., 2009; Lessard et al., 2007; Yan et al., 2008).

To investigate the function of BAF170 during cortical neurogenesis, we generated and analyzed cortex-specific, conditional *BAF170* knockout (cKO) and overexpressing (cOE) transgenic mice. Our data reveal that *BAF170* acts within a precise time window to repress indirect cortical neurogenesis, and control cortical size. We show here that BAF170 globally suppresses the expression of Pax6 target genes, including those with known functions in regulating the proliferation and specification of both IPs and late progenitors (LPs), cells that are predominantly involved in the generation of neurons with upper layer identities. As a part of the mechanism involved, we show that during the period of early neurogenesis, by competing with BAF155 subunit in mSWI/SNF, BAF170 controls euchromatin structure, and represses Pax6 target genes by directly recruiting the REST

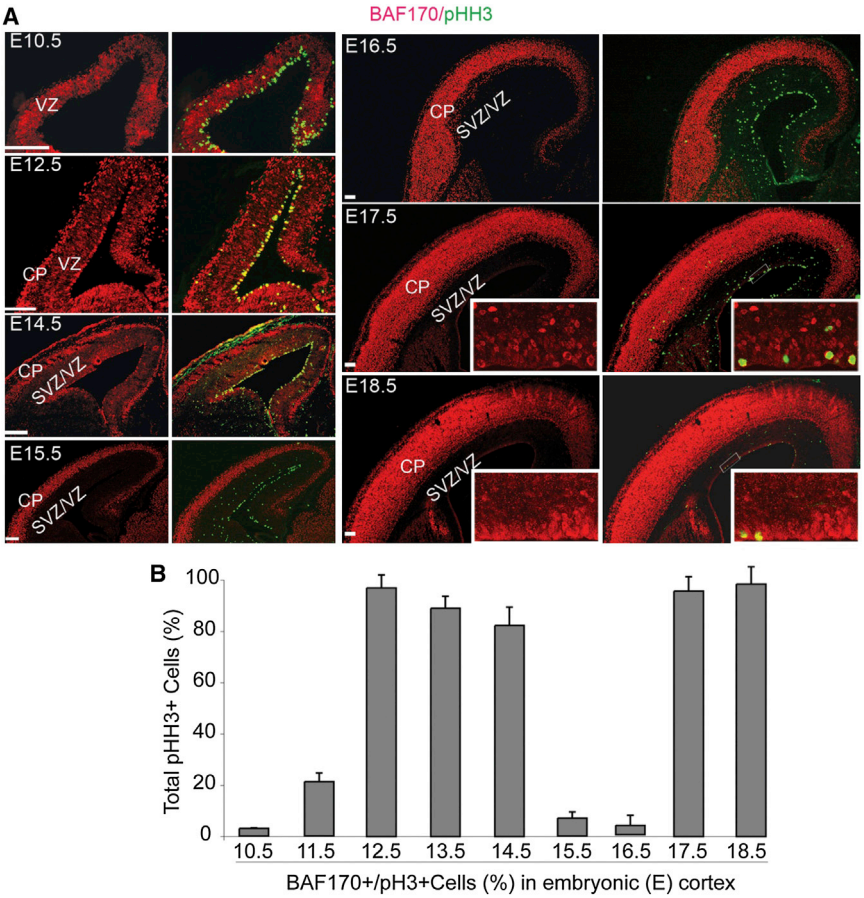

Figure 1. Temporal Expression of BAF170 in Cortical Progenitors

(A) Images show single or double immunolabeling with antibodies for BAF170 (red) and pHH3 (green) at the indicated mouse embryonic stages.

(B) Estimate of the percent of all of pHH3$^+$ cells that are double-positive for BAF170 and pHH3 in developing cortex. The counting was done on the picture, including the entire sections. Statistical analyses were done using Student's t test. Values are presented as means ± SEM (n = 4). Scale bars represent 250 μm.

See also Figure S1.

(RE1-silencing transcription factor)-corepressor complex to their promoters.

RESULTS

Expression of BAF170 in Developing Mouse Cortex

To investigate the dynamics of BAF170 expression, we performed double immunohistochemical (IHC) analysis on coronal brain sections of control animals at embryonic stages (E) E10.5–E18.5 using antibodies against BAF170 and phospho-histone 3 (pHH3), a marker for cycling cells in M and late G2 (Weissman et al., 2003). During early neurogenesis (E10.5–E14.5), BAF170 is strongly expressed in cortical progenitor cells, whereas at E15.5–E16.5 the expression is almost absent in the progenitors, but kept in postmitotic cells of the cortical plate (CP) (Figure 1A and Figure S1A available online). Notably, BAF170 expression reappears in the VZ at the beginning of cortical gliogenesis (E17.5–E18.5), as well as in the postnatal and adult niches of brain neurogenesis: the forebrain SVZ and the hippocampal dentate gyrus (DG) (Figure 1 and data not shown).

At E12.5–E14.5, a period of peak IP production, we found that most pHH3$^+$ cells, including those at the apical and basal surface of the VZ, expressed relatively high levels of BAF170 (Figures 1A and 1B). A small proportion of pHH3$^+$ cells (4% ± 0.9% at E12.5, 7% ± 0.7% at E13.5, and 11% ± 1.3% at E14.5) in close proximity to the apical surface (which likely are in G2 phase), were negative for BAF170 (Figure S1A). To better address this issue, we performed in vivo labeling of cortical progenitors with CidU for 6 hr and IdU for 2 hr and looked for cells in S or G2 phases of the cell cycle (CidU$^+$/IdU$^+$ and CidU$^+$ cells, respectively). Triple IHC for BAF170, CidU and IdU revealed that BAF170 is not expressed in either S or G2 phase cells (Figure S1B).

As reported previously (Pinto et al., 2008), a fraction of prominin-positive RGCs characterized by low activity of the human glial fibrillary acidic protein (hGFAP) promoter is largely restricted to the generation of neurons via the direct mode of neurogenesis. In contrast, prominin$^+$ RGCs with a highly active *hGFAP* promoter generate nonneuronal progeny and produce neurons indirectly, via IPs. To determine which of these RGCs subtypes BAF170 is present in, we performed triple IHC with BAF170, prominin, and Cre antibodies on coronal brain sections of the *hGFAP-Cre* mouse line in which the *hGFAP* promoter drives expression of Cre (Zhuo et al., 2001). We found that at E13.5, BAF170 is mainly expressed in the prominin$^+$/Cre^{high} RGC fraction (87% ± 3.2%) at the ventricular apical surface, whose progeny are Tbr2$^+$ IPs (Figure S1C) (Pinto et al., 2008). Thus, in the time window E12.5–E14.5, BAF170 is expressed exclusively in the nonneurogenic RGCs involved in the indirect mode of neurogenesis.

BAF170 Controls Total Cerebral Cortical Volume

The *BAF170* full KO, generated through crossing of *BAF170fl/fl* with a ubiquitous deleter *CMV-Cre* mouse line, resulted in a slightly increase of the body weight at stage E13.5. However, the animals died shortly after birth (P0–P3, data not shown). Therefore, to address the functions of BAF170 in corticogenesis in vivo, we generated transgenic mice in which *BAF170* was conditionally deleted (cKO) or overexpressed (cOE) in the developing cortex (Figures S2A–S2G). Both cKO and cOE mice were viable, healthy, and fertile. To accurately measure the effect of both genetic manipulations on cortical size, we used in vivo structural MRI. This stereological method allows the quantification of volume changes of specific brain structures without

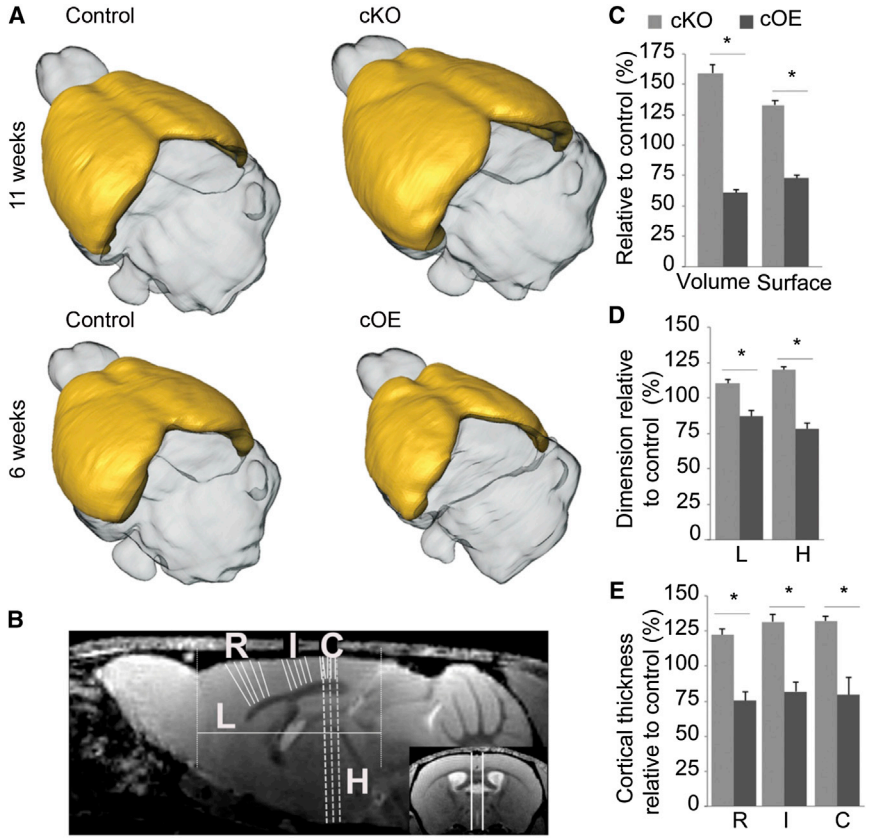

Figure 2. BAF170 Controls Cortical Size

(A) Three-dimensional reconstruction of magnetic resonance imaging (MRI) data sets of the analyzed brain and cortex (in yellow) parameters of control, *BAF170*cKO and *BAF170*cOE mice.

(B–E) Statistical analyses comparing parameters of cortical size in *BAF170*cOE, *BAF170*cKO (relative to control) as presented in (B). Abbreviations: length of dorsoventral (H), rostrocaudal (L) forebrain and thickness of rostral (R), intermediate (I), and caudal region (C) cortex. Five animal pairs Mutant/Control (from the same litter) for each condition were tested at age of 6 and 11 weeks. Asterisks refer to statistically significant differences ($p < 0.05$) according to the Mann-Whitney test.

See also Figures S2H–S2J.

shrinking artifacts caused by chemical fixation, becoming therefore a standard for anatomical studies in both human and mice. The volume and the surface area of the neocortex in *BAF170* loss-of-function (LOF) mutants were increased by 60% and 30%, respectively, whereas these two parameters were diminished in *BAF170*cOE mice by 39% and 27%, respectively (Figures 2A–2C). As illustrated in Figure 2E, *BAF170*cKO mice had enhanced cortical thickness by 22% in the rostral area (R), by 32% in the intermediate area (I), and by 32% in the caudal area relative to the control. In contrast, in *BAF170*cOE mice the cortical thickness in the corresponding sections was reduced by 25% (R), 18% (I), and 21% (C). Changes in neocortical volume were accompanied by an increase (by 22%) and a reduction (by 22%) of the anterior-posterior dimension (L-value) in *BAF170*cKO and *BAF170*cOE, respectively (Figure 2D). In addition, the dorsoventral dimension (height) of the brain was increased in *BAF170*cKO and reduced in *BAF170*cOE mice (Figure 2D). However, in *BAF170*cKO, the brain height excluding the cortex (H-C value, Figures 2B) did not differ significantly from those of controls and the cortical thickness was significantly increased relative to the dorsoventral dimension of the brain (Figure S2J, upper diagram). Noteworthy, the results were consistent at different levels along the cortical anterior-posterior axis showing a very low variation in measurements in the tested five pairs (control versus mutant) in both paradigms, *BAF170*cKO and *BAF170*cOE. Together, these results show that the expression level of *BAF170* is critical for determining overall cortical volume and thickness.

Loss of BAF170 Promotes Indirect Neurogenesis

In *BAF170*cKO mice, both the identity and proliferation of progenitor cells at the apical VZ surface appeared normal, based upon their expression of the RGC-specific TF Pax6 and labeling with the mitotic maker pHH3 (Figures S3A and S3B). Strikingly, however, the *BAF170c*KO cortex contained twice as many nonapical pHH3$^+$ cells as controls, suggesting that BAF170 can influence IP pool size through its specific expression in the nonneurogenic RGCs (Figure S1D).

We next investigated the generation of IPs in the BAF170 LOF cortex by analyzing the expression of TF Tbr2, necessary for IP identity (Hevner et al., 2006). At E12.5, the number of Tbr2$^+$ cells was significantly increased in the SVZ of the *BAF170* deficient cortex, becoming progressively increased during the period E13.5–E15.5 (Figures 3A and 3B). The expression of other genes expressed in IPs, including *Cux2, Svet1*, was also greatly upregulated in E14.5 *BAF170*cKO cortices (data not shown). Despite the greatly increased number of Tbr2$^+$ IPs, BAF170 deletion did not affect the ratio of pHH3$^+$ IPs to total Tbr2$^+$ IPs (Figure S3C), indicating that the proliferative capacity of the IPs was unaffected.

To determine whether *BAF170* LOF affects proliferation and cell cycle exit of progenitor cells, we performed 24 hr BrdU pulse labeling of cycling cortical progenitor cells in vivo. Double IHC with antibodies for BrdU and Ki67, a marker for proliferating progenitors in all except for G2 phase of the cycle, revealed a significantly lower cell cycle exit index in *BAF170cKO* cortex than in the controls (Figures S3D and S3E). Together, these results strongly suggest that in absence of BAF170 the RGPs are biased to asymmetric nonneurogenic divisions, and hence to self-renewal and the production of IPs, instead of neurons (RGC = RGC + IP). In further support of this hypothesis, at E12.5–E13.5, IHC and qRT-PCR for Tuj1, a general neuronal marker, and Ctip2, a marker of early-born, deep (lower) layer neurons, revealed a substantial reduction in cell density and level of expression of these neuronal subsets that

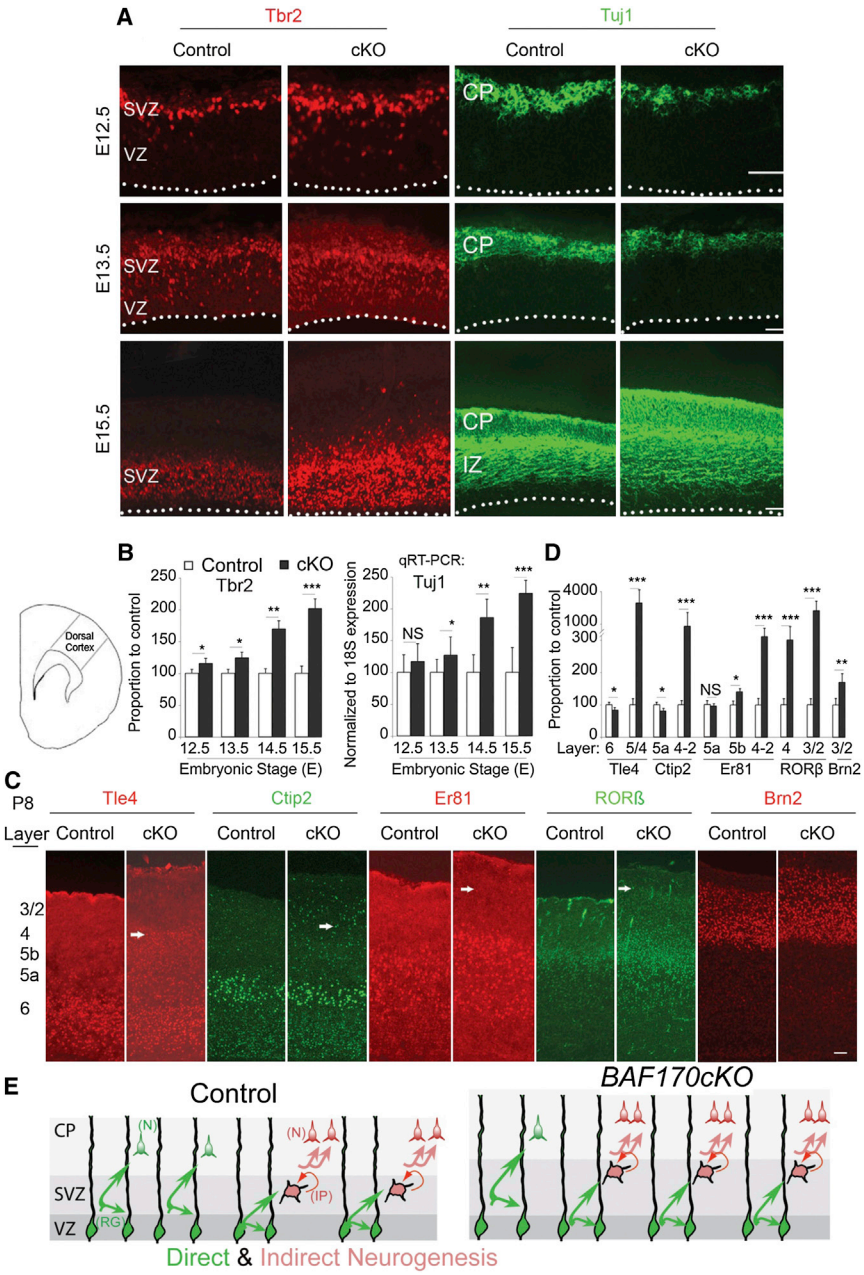

Figure 3. Loss of BAF170 Promotes Indirect Neurogenesis and Causes Cortex Thickening and Defects in Cortical Layering

(A) IHC analyses with antibody markers for IPs (Tbr2) and neurons (Tuj1) on coronal sections of E12.5, E13.5, and E15.5 within a field of the dorsal cortex at the level of septum as indicated in the schema.

(B) Quantitative analysis of the number of Tbr2$^+$ IPs and qRT-PCR analysis of *Tuj1* transcripts in *BAF170*cKO compared to control cortices at E12.5–E15.5. Counting was done in frames (350 μm × 250 μm) of digitalized pictures, shown in (A). Statistical analyses were done using Student's t test. Values are presented as means ± SEM (n = 4 for Tuj1; n = 8 for Tbr2).

(C) IHC analyses of cortical phenotype at postnatal stage P8 with layer-specific markers in somatosensory area. White arrows show ectopic positions of LL neurons in the ULs.

(D) Analyses of the number of layer-specific neurons (shown in C) of *BAF170*cKO compared to control mice. The field for counting (300 μm × 900 μm) is pointed by a frame, SS, in Figure S4D. Scale bars represent 50 μm (A, E12.5 and E13.5), 100 μm (A, E15.5) and in (C) (P8).

(E) Schema illustrating that in a lack of BAF170, a higher proportion of RGCs exert nonneurogenic (RGC = RGC + IP) asymmetric division, promoting the indirect mode of neurogenesis.

See also Figures S3 and S4.

are generated by early neurogenic RGCs. However, by midcorticogenesis differences in the expression of Tuj1 (E14.5) and Ctip2 (E14.5–E15.5) were no longer significant, and subsequently at E15.5 a much thicker band of Tuj1$^+$ neurons was detected in the intermediate zone (IZ) and CP of the *BAF170*cKO cortex (Figures 3A and 3B; data not shown). In addition, at E15.5 the expression of Satb2$^+$, an upper layer-specific transcription factor, was strongly enhanced in the *BAF170*cKO (176% ± 18%) compared to the control cortex (100% ± 13%; Figures S3F and S3G).

To investigate the function of BAF170 in postmitotic neurons, we generated a neuron-specific *BAF170*KO using the *Nex-Cre* line as a driver (Goebbels et al., 2006). The selective elimination of BAF170 in postmitotic neurons had no effect on the number of cortical progenitors or neuronal production (Figures S3H and S3I), indicating that postmitotic expression of *BAF170* does not significantly influence RGP proliferation or neuronal differentiation.

To investigate further how *BAF170* influences the mode of neurogenesis, we performed in vivo experiments using in utero electroporation to acutely delete BAF170 from individual cells. Brains of E13.5 *BAF170fl/fl* embryos were electroporated either with pCIG2-Cre-ires-eGFP (Cre-eGFP) or control pCIG2-ires-eGFP (eGFP) plasmids (Figures S4A–S4C). At midgestation, RGCs undergo only one division in 24 hr. To study the fate of RG daughter cells, we performed triple immunostaining for GFP, Tuj1, and Tbr2 at E14.5. In the control, electroporated (eGFP$^+$) cells were located in the SVZ/IZ and some coexpressed Tuj1 (18% ± 2.5% of all GFP$^+$ cells), representing differentiated neurons generated directly from either RGCs (white filled arrows, Figure S4B1) or Tbr2$^+$ IPs (white empty arrows, Figure S4B3). By comparison, following the acute deletion of *BAF170*, we found only a very small number GFP$^+$/Tuj1$^+$ cells (0.5%) (filled arrows, Figures S4B2 and S4C). In contrast, the number of GFP$^+$/Tbr2$^+$ cells (IP fate) was increased in Cre-eGFP-injected cortices (57% ± 6%) as compared to control (32% ± 4%) (empty arrows, Figures

S4B3, S4B4, and S4C). As the ratio of nonapical pHH3$^+$ IPs to total Tbr2$^+$ IPs was not affected in the E14.5 *BAF170*cKO cortex (Figure S3C), these data confirm that loss of BAF170 biases asymmetrically dividing RGPs to self-renewal and the generation of IPs.

To investigate the final numbers of cortical neurons produced in the *BAF170* null cortex and their laminar positions, we analyzed the expression of layer-specific genes and proteins at postnatal day 8 (P8). Consistent with the results of our in vivo MRI study, immunostaining for Tbr1, which at this stage delineates both LL and UL neuronal subtypes, revealed a significant increase in radial thickness at both rostral and caudal levels, specifically affecting the ULs of *BAF170*cKO cortices (Figures S4D and S4F). In contrast, staining for L6 and L5 neuronal markers (Molyneaux et al., 2007) revealed a slight reduction of the number of FoxP2$^+$, Tle4$^+$, Ctip2$^+$, and Er81$^+$ LL neuronal cell types at their normal positions in *BAF170*cKO. Notably, sets of LL neurons were ectopically present within the ULs (Figures 3C and 3D). In addition, the expression of TAG1 that selectively stains corticofugal interhemispheric axonal projections in the dorsal domain of corpus callosum was also enhanced (by 124.8% ± 4.7% at the rostral and 132.1% ± 6.2% at caudal level, compared to the control (100% ± 5.8% at rostral and 100% ± 5.6% at caudal level) (Figure S4G). Finally, *BAF170*cKO mice have no gross migration or apoptosis defects as assessed by BrdU-birth dating of neurons and cleaved Caspase3 IHC (Figure S4H; data not shown).

Collectively, these findings suggest that the loss of *BAF170* function drives RGCs to prematurely switch to the indirect mode of neurogenesis, by increased generation of IPs (Figure 3E). This causes three main defects in the postnatal *BAF170*cKO cortex: (1) slightly reduced presentation of LL neuronal types at their normal locations, (2) ectopic expansion of neurons with LL identity into UL locations, and (3) a strikingly increased output of neurons with UL identity (Figure 3E).

Overexpression of *BAF170* Induces Direct Neurogenesis

To further investigate whether BAF170 has an instructive role in regulating direct versus indirect neurogenesis, we studied the effect of overexpressing *BAF170* in cortical progenitors in transgenic BAF170 gain-of-function (GOF) (designated as *BAF170*cOE) mice (Figure 4). In those mice, we found a cortical phenotype opposite to that of the *BAF170*cKO mice: in *BAF170*-cOE embryos the number of Tbr2$^+$ IPs at E12.5–E13.5 was substantially diminished, and the early CP contained an increased number of Tuj1$^+$ neurons. Subsequently, at E14.5–E15.5, the number of neurons in the CP was decreased compared to controls (Figures 4A and 4B). Analysis of the neuronal layer distribution in *BAF170*cOE at P10 revealed a diminished radial thickness that more severely affected the width of the upper layers, and a slight increase in neuronal density in L6 (Figures 4C, 4D and S5). Thus, by promoting the early direct mode of neurogenesis (RGC = RGC + N) expression of *BAF170* appears to determine the final neuronal outcome for distinct cortical layers (Figure 4E). Together, these findings suggest that at early stages (E12.5–E14.5), the expression of BAF170 in M phase nonneurogenic RGCs prevents a premature switch toward the indirect mode of neurogenesis.

Control of Cortical Size by BAF170 Involves Suppression of Pax6 Transcriptional Activity

Induction of neural progenitor fate in ESCs is accompanied by transcription of BAF170 and Brm subunits (Ho et al., 2009; Lessard et al., 2007; Yan et al., 2008), and of Pax6 (Gajović et al., 1997). Strikingly, the cortical phenotypes of cortex-specific *BAF170*cKO (this study) and *Pax6*cKO mice (Georgala et al., 2011; Tuoc et al., 2009) are the opposite of one another, in terms of cortical growth and neuronal layer production. These findings prompted us to investigate a possible interaction between BAF170 and Pax6. IHC revealed coexpression of BAF170 and Pax6 in RGCs in the VZ of the developing cortex (Figure S6A). Moreover, coimmunoprecipitation assays with either BAF170 or Pax6 antibodies found that Pax6 does indeed interact with multiple BAF subunits, including BAF170, BAF155, and Brm in cortical progenitors (Figure 5A).

As the transcriptional program regulated by Pax6 in the early cerebral cortex has been previously characterized (Sansom et al., 2009), in order to gain insight into the interaction between BAF170 and Pax6, we performed a transcriptome analysis of the changes in gene expression in the E12.5 cortex of *BAF170*cKO embryos. We identified significant changes in cortical gene expression, detecting 875 up- and 1,033 downregulated genes (Table S1; Figures 5B, S6B, and S6C). Gene ontology (GO) analysis of these genes revealed a significant enrichment for genes involved in chromatin regulation, neurogenesis and forebrain development, including *Tbr2* (Sessa et al., 2008), *Cux1* (Cubelos et al., 2008), *Tle1* (Buscarlet et al., 2008), *Ngn2* (Bertrand et al., 2002), *AP2*γ (Pinto et al., 2009), and *Er81* (Tuoc and Stoykova, 2008a) (Table S1; Figures S6B and S6C).

We then performed a transcriptome level analysis of the interaction between BAF170 and Pax6 by comparing genes regulated by BAF170 in the *BAF170*cKO cortex with genes previously shown to be regulated by Pax6 in the Pax6-overexpressing (*D6-Pax6* transgenic) or *Pax6* mutant (*Sey/Sey*) E12.5 neocortex (Sansom et al., 2009). We found a significant overlap, approximately twice that expected by chance ($p < 1 \times 10^{-16}$, hypergeometric test), between the set of genes with altered expression in *E12.5 BAF170*cKO cortex and the set of genes regulated by *Pax6*. Notably, BAF170 represses the majority of genes positively regulated by Pax6 (Figure 5B; Table S1).

We next asked whether the interaction of BAF170 with Pax6 influences Pax6-dependent transcriptional activity using a Pax6-dependent reporter construct (pCON/P3), in cortical NSCs from *BAF170*cKO and control mice. The loss of BAF170 profoundly potentiated pCON/P3 reporter activity in cultured cortical NSCs (Figure 5C). However, BAF170 did not prevent Pax6 binding to its consensus sequence (Figure S6D), suggesting that BAF170 may recruit a repressor to Pax6 target genes. Therefore, we sought to study whether BAF170 influences the expression of three Pax6 target genes, *Tbr2*, *Cux1*, and *Groucho/Tle1* (Sansom et al., 2009) that are known to be expressed in, and involved in the specification of IPs/late progenitors (LP), and upper layer neurons (Molyneaux et al., 2007). In addition to increased number of Tbr2$^+$ IPs (Figures 3A and 3B), the loss of BAF170 also led to an increase in the expression of Tbr2 in IPs, as revealed by a greater density of the IHC signal in cKO cortices compared with the controls (Figure 5D). IHC analyses also indicated that *BAF170*LOF caused prematurely high

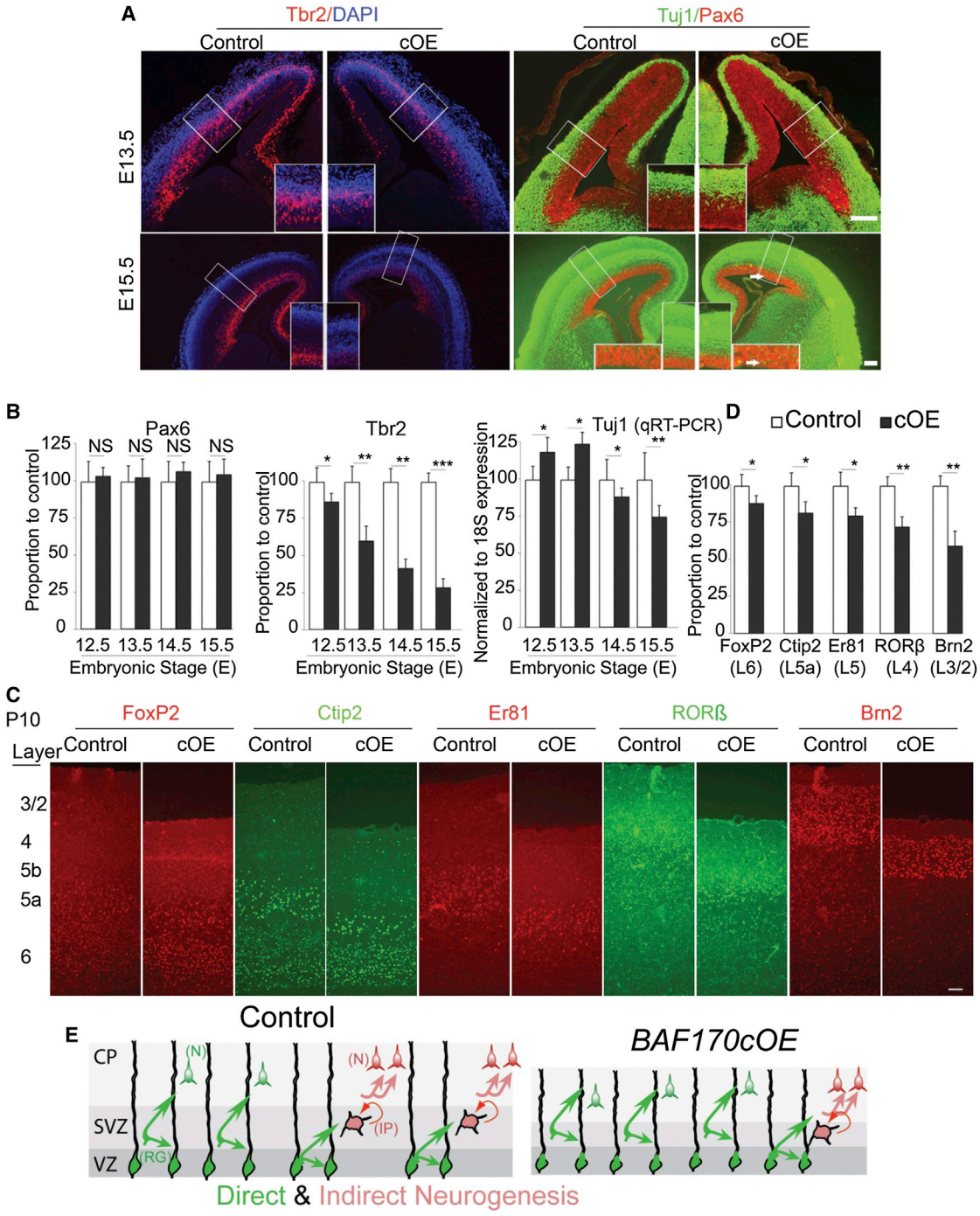

Figure 4. Activation of *BAF170* Promotes the Direct Neurogenesis and Leads to a Reduction in the Thickness of All Cortical Layers

(A) IHC analyses with antibodies specifically labeling RGCs (Pax6), IPs (Tbr2), and neurons (Tuj1) on matched cross E13.5 and E15.5 brain sections from control and *BAF170*cOE embryos. White arrows show ectopic presence of Tuj1$^+$ neurons in the VZ. The medially located picture insets are higher magnification images from the fields (350 μm × 250 μm) in which the counting was done (indicated by white frames in cortex).

(B) Statistical analyses of IHC assay (shown in A) comparing the number of Pax6$^+$ RGCs, Tbr2$^+$ IPs (left two diagrams) and results (right diagram) from qRT-PCR analysis of *Tuj1* transcripts in control and *BAF170*cOE cortices at E12.5–E15.5.

(C and D) IHC (C) and quantitative (D) analysis of the number of neuronal subsets labeled by layer-specific markers in presumptive somatosensory area (SS) in control and *BAF170*cOE cortices at P10 (SS, as selected frames of 300 μm × 900 μm in Figure S4D).

(E) Schema illustrating that upon overexpression of BAF170, a higher proportion of RGCs undergo neurogenic (RGC = RGC + N) asymmetric division, promoting the direct mode of neurogenesis. Statistical analyses were done using Student's t test. Values are presented as means ± SEM (n = 4). Scale bars represent 250 μm.

See also Figure S5.

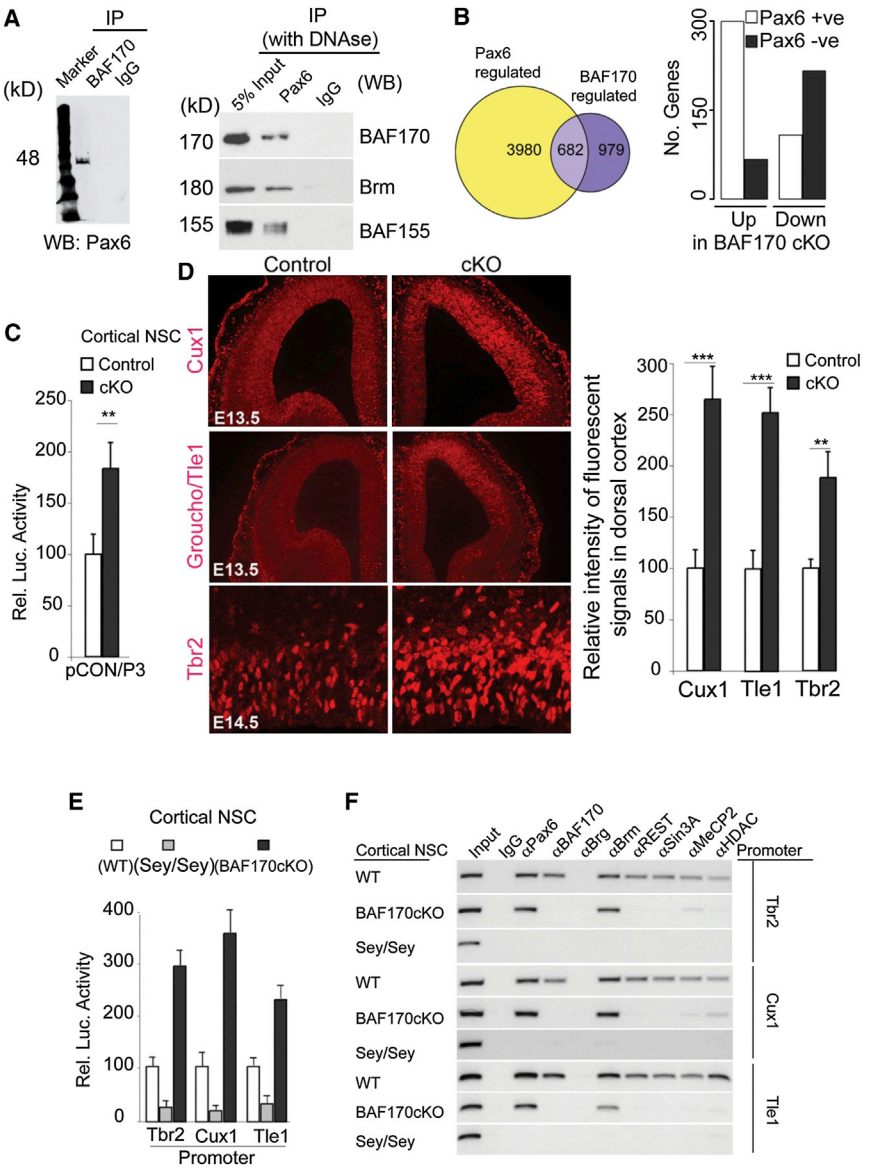

Figure 5. BAF170 Recruits the REST-Corepressor Complex to Pax6 Downstream Promoters

(A) Immunoprecipitation and western blot experiments demonstrate that Pax6 interacts simultaneously with BAF170, BAF155, and Brm in E13.5 cortical progenitors.

(B) Genes with a changed expression in E12.5 *BAF170*cKO cortex significantly overlap (approximately twice as many genes as expected by chance, $p < 1 \times 10^{-16}$, hypergeometric test) with genes previously shown to be regulated by Pax6 (Sansom et al., 2009). "Pax6+ve" and "Pax6-ve" are numbers of genes positively regulated and negatively regulated by Pax6, respectively. Notably, BAF170 represses the majority of genes positively regulated by Pax6.

(C) Promoter-reporter assay was performed with *Pax6*-dependent luciferase reporter in cultured NSC from control and cKO cortices. Note that the loss of *BAF170* function potentiates Pax6-dependent transcriptional activity.

(D) IHC and statistical analyses reveal in the *BAF170*cKO cortex at E13.5 a developmental premature upregulation of the expression *Cux1*, *Tle1*, and *Tbr2*, three Pax6 target genes involved in specification of late progenitors and IPs.

(E) Promoter-reporter assays for *Tbr2*, *Cux1*, and *Tle1* performed in cortical NSCs from indicated sources.

(F) ChIP analyses of the in vivo occupancy of *Tbr2*, *Cux1*, and *Tle1* promoters in NSCs using indicated antibodies. Statistical analyses were done using Student's t test. Values are presented as means ± SEM (n = 4). Scale bars represent 250 μm.

See also Figure S6.

expression of both *Cux1* and *Tle1* in the VZ/SVZ as early as E13.5 (Figure 5D).

We next studied the effect of endogenous Pax6 and BAF170 levels on the activity of *Tbr2*, *Cux1*, and *Tle1* promoter-reporter constructs. Neural stem cultures (NSC) from E12.5 cortices from control, homozygous *Pax6*/*Small eye* mutant (*Sey*/*Sey*) and *BAF170cKO* embryo brains were transfected with luciferase reporter constructs for each of the three genes and analyzed after 2 days (2 DIV). Notably, we found opposite effects on the reporter activities in the different genetic backgrounds, with reporter activity almost abolished in *Sey*/*Sey* but dramatically increased in *BAF170c*KO NSC cultures (Figure 5E). Thus, Pax6 and BAF170 appear to exert opposing effects on the expression of these Pax6 target genes involved in IP/LP genesis (Cubelos et al., 2008; Sessa et al., 2008).

To understand the basis for these protein interactions, we examined the in vivo occupancy of the *Tbr2*, *Cux1*, and *Tle1* promoters in NSCs. Using chromatin immunoprecipitation (ChIP) assays, we found that Pax6 bound to the promoters of the three targets, consistent with previous data (Figure 5F). Remarkably, BAF170 also occupied all three promoters in wild-type NSCs, but not in *Sey*/*Sey* NSCs lacking Pax6 (Figure 5F). Although Pax6 was essential for the binding of Brm to the three targeted promoters, we did not detect the presence of Brg1 on these promoters (Figure 5F). Moreover, we found the Brm and Brg proteins to be located in distinct nuclear regions of cortical progenitors, suggesting that they occupy different chromatin locations (data not shown). Collectively, these findings suggest that BAF170 and Brm, present in the same BAF complex, interact with Pax6 and together occupy the promoters of the Pax6 downstream target genes *Tbr2*, *Cux1*, and *Tle1*.

The transcriptional repressor REST binds to RE1 elements in the regulatory regions of many neuron-specific genes, negatively regulating transcription in nonneural tissues and NSCs (Ballas et al., 2005; Chen et al., 1998) by recruiting multiple corepressors, including CoREST, HDAC1, HDAC2, CoREST, MeCP2, and Sin3 (Lunyak et al., 2002). REST interacts with multiple BAF subunits, including BAF170 and Brm (Ballas et al., 2005; Battaglioli et al., 2002) Therefore, we studied whether the

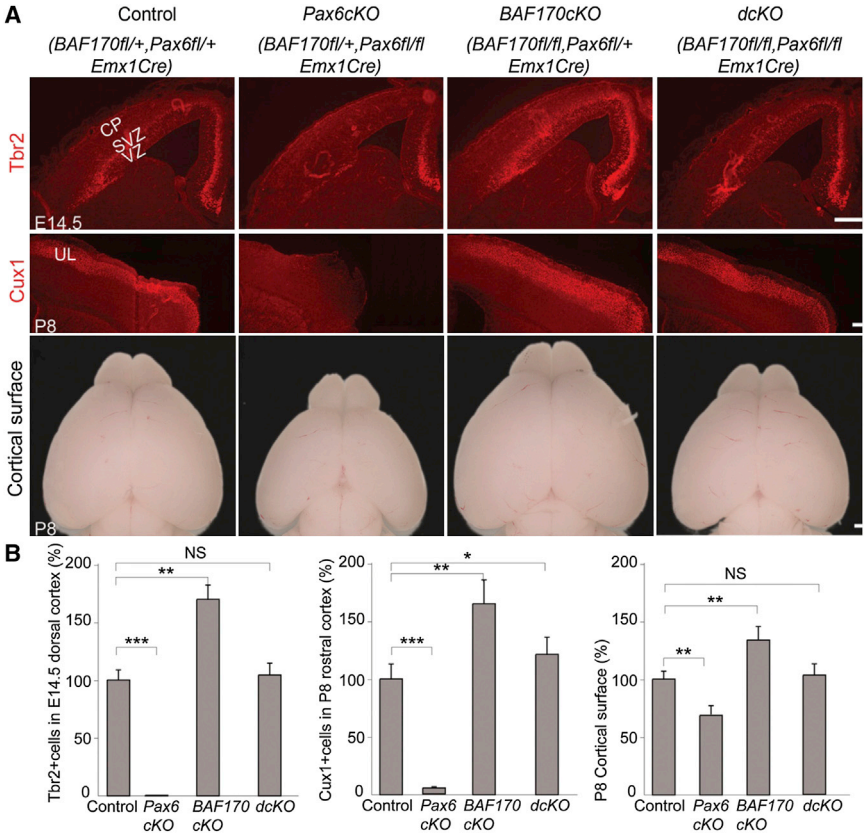

Figure 6. Genetic Interaction between Pax6 and BAF170 Controls Cerebral Cortical Size

Histological (A) and quantitative (B) analyses of the number of Tbr2$^+$ IPs, Cux1$^+$ UL neurons, and size of cortical surface in *Pax6*cKO, *BAF170*cKO, and double *Pax6*cKO;*BAF170*cKO (dcKO) cortices as compared with controls at E14.5 and P8. The counting was done on digitalized pictures, including entire sections. Statistical analyses were done using Student's t test. Values are presented as means ± SEM (n = 4, except for cortical surface n = 3). Scale bars represent 500 μm.

REST-corepressor complex also occupies the *Tbr2*, *Cux1*, and *Tle1* promoters in NSCs. Using antibodies that recognize different components of the complex, we found that all of the components of the REST-corepressor complex studied show association with promoter regions of *Tbr2*, *Cux1*, and *Tle1*. Notably, in the absence of BAF170 (in *BAF170*cKO NSC) or Pax6 (in *Sey*/*Sey* NSC), REST-complex binding to these three promoters was either completely abolished or significantly reduced (Figure 5F), suggesting that Pax6 together with BAF170 mediates REST-corepressor complex binding to *Tbr2*, *Cux1*, and *Tle1* promoters (Figure 5F).

Recent data suggested that the silencing of CoREST leads to an increased number of IPs in developing cortex (Fuentes et al., 2012). Therefore, we investigated whether a reduction in REST level has consequences for IP genesis. Using two effective shRNA constructs for *REST* (shREST#1, shREST#2) we performed in utero electroporation of either shREST plus GFP plasmids or GFP plasmid alone (as a control) into E13.5 brains of same littermates. In control, GFP-electroporated cortices at E15.5, a large population of GFP$^+$ cells had migrated into the IZ/CP, and many GFP$^+$ cells were still present in the VZ/SVZ (Figures S6E and S6F). However, in cortices electroporated with GFP plus shREST constructs, most GFP$^+$ cells were located in the SVZ and IZ, with only few GFP$^+$ cells remaining in VZ (Figure S6E). We examined the fate of the progeny of the electroporated cells using double IHC with antibodies for GFP, Pax6 (RGPs), Tbr2 (IPs), and HuC/D (neurons) (Figure S6E). We found that cortices electroporated with GFP plus shREST contained many fewer double-labeled GFP$^+$/Pax6$^+$ RGCs (5.2% ± 0.7% with shREST#1 and 6.1% ± 0.8% with shREST#2) compared with GFP-treated controls (34% ± 4.7%) (Figures S6E and S6F). Furthermore, the number of GFP$^+$/Tbr2$^+$ positive cells (IPs) was significantly increased in GFP plus shREST-injected brains (28.1% ± 3.2% with shREST#1 and 25.2% ± 3.5% with shREST#2) compared to the GFP-treated cortices (17.5% ± 028%) (Figures S6E and S6F). In addition, the number of GFP$^+$/HuCD$^+$ cells in GFP plus shREST-injected cortices (67% ± 4.9% with shREST#1 and 65% ± 5.1% with shREST#2) was greater than that in GFP alone-injected cortices (49% ± 4.7%) (Figures S6E and S6F). In agreement with Fuentes et al., (2012), these findings indicate that REST and coREST play an important role in the genesis of IPs.

To investigate whether the *BAF170*LOF phenotype (enhanced number of Tbr2$^+$ IPs, thicker Cux1$^+$ ULs, and enlarged cortical surface) could be rescued by loss of Pax6 function, we generated double *BAF170*cKO/*Pax6*cKO mice (referred to as dcKO, Figure 6). We found that cortical surface at P8 in the dcKO animals was similar to the controls, and the number of Tbr2$^+$ IPs at E14.5 in both genotypes was almost equal (499.5 ± 15.9 in dcKO cortex compared to 478% ± 11.73% in control cortex; Figure 6B), suggesting that loss of Pax6 function almost fully reduced the excessive generation of Tbr2$^+$ IPs seen in the *BAF170*LOF cortex. We noticed, however, that dcKO cortices still showed an increased production of Cux1$^+$ UL neurons (3,411.5 ± 188) compared to controls (2,813.5 ± 130.92), suggesting that BAF170 controls production of UL neurons through additional mechanisms (Figure 6B).

Competition between BAF170 and BAF155 Affects Chromatin Modifications and Binding of the Pax6/REST-Corepressor Complex to Pax6 Target Promoters

Neural induction in ESCs is accompanied by the replacement of one BAF170 subunit with BAF155 in the mSWI/SNF complex (Ho et al., 2009; Yan et al., 2008). At E12.5, both BAF155 and BAF170 are detectable in the progenitor cells of the VZ (Figure S7A). However, at E15.5, the peak of late indirect neurogenesis, BAF170 and BAF155 show complementary expression

patterns: while the expression of BAF170 is almost absent from RGPs, BAF155 is highly expressed (Figure S7A).

To study whether BAF170 expression could influence the expression of BAF155, we performed IHC and western blot analyses of tissue samples from E14.5 and P8 cortices of *BAF170*cKO and *BAF170*cOE mice. Interestingly, loss of BAF170 in E14.5 *BAF170cKO* cortex led to upregulation of BAF155 expression, and only a slight reduction of BAF57, whereas other main subunits of the BAF complex (Brm, Brg, BAF45a, BAF53a) remained unaltered (Figures S7B and S7C). In contrast, overexpression of BAF170 via electroporation of a BAF170-eGFP plasmid into E14.5 embryo brain resulted in the abrogation of BAF155 expression (Figure 7A), which is similar to what has been reported in ESCs (Ho et al., 2009). These findings suggest that BAF170 expression controls mSWI/SNF composition by affecting the expression of the BAF155 subunit.

As shown in Figure S7E, at least two BAF170 proteins per BAF complex appear to be present in cortical progenitors. Interestingly, both *BAF170* LOF and GOF affected neither the transcription nor the promoter activity of BAF155 (Figure 7A). In addition, we were able to show an interaction between REST protein and BAF170 by coimmunoprecipitation, as previously reported (Battaglioli et al., 2002), but could not find an interaction between the BAF155 and REST proteins in a cell culture system (Figure 7B). To map the region of BAF170 that interacts with REST, we used a series of Flag-tagged BAF170 deletion constructs and expressed them in HeLa cells (Figure 7B, scheme). In Flag pull-down assays of REST-transfected HeLa cell lysates, REST was found to interact with BAF170 fragments that included the C170 domain, but not with constructs that lacked the C170 domain (Figure 7B). Notably, we observed considerable differences between the amino acid (aa) sequences of BAF170 and BAF155 at the C terminus (C170 and C155) (Figure S7F). These data suggest that the different binding capacity of BAF155 and BAF170 to REST is due to the difference in aa sequence at the C-terminal of two proteins. Together, these results imply that the loss of BAF170 in the *BAF170*cKO cortex results in the incorporation of additional BAF155 subunit(s) into the SWI/SNF complex, leading to the elimination of the REST-dependent corepressor complex in cortical progenitors.

Immunoprecipitation experiments revealed that in addition to BAF170, Pax6 also interacts with BAF155, suggesting that *BAF170*LOF and GOF should influence the enrichment of BAF155 on the promoters of Pax6 target genes. Indeed, we found this to be the case with *BAF170* knockout and overexpression leading to opposing effects, namely the enrichment or abolishment of BAF155 on the assayed promoters of *Tbr2*, *Cux1*, and *Tle1* (Figure 7C).

Recent evidence indicated that BAF155 alone or together with Brg1 facilitates ES cell reprogramming by promoting euchromatin formation (Singhal et al., 2010). We therefore examined repressive (H3K27Me3) and active (H3K9Ac) chromatin marks on the promoters of *Pax6/BAF170* target genes in both the *BAF170*LOF and *BAF170*GOF cortex (Figures 7D and 7E). Although global levels of the H3 modification were unchanged (Figures S7G and S7H), *BAF170* LOF resulted in an increase in active chromatin marks on *Cux1* and *Tle1* promoters with a complementary reduction in repressive modifications, whereas *BAF170*GOF had the opposite effect (Figures 7D and 7E).

We also performed bisulfite sequencing to study CpG methylation (repressive marks) on the *Cux1* and *Tle1* promoters using genomic DNA isolated from control and *BAF170*cKO cortices, or E14.5 cortices electroporated at E13.5 with the expression plasmids for: BAF170 alone, a combination of BAF170 and BAF155 (1:1), or of BAF170 and Pax6 (1:1) (Figure 7F). We found a marked decrease of CpG methylation in the *BAF170* cKO, and an increase upon *BAF170* overexpression as compared with that in controls. This phenotype was partially rescued upon cotransfection with both *BAF170*/*BAF155* expression plasmids, but not with *BAF170*/*Pax6* plasmids (Figure 7F). These results indicate that the competition between BAF170 and BAF155 subunits is essential for epigenetic/chromatin status and the expression of late progenitor genes during corticogenesis.

We next examined whether changes in chromatin modification status influenced binding of Pax6 to its target promoters in ChIP assay. Interestingly, *BAF170*LOF and GOF significantly enriched and diminished Pax6 binding to the *Cux1* promoter, respectively, and tended to have similar effects on the *Tle1* promoter (Figure 7G).

From these data we conclude that, during early neurogenesis (up to E14.5), Pax6 interacts with both BAF155 and BAF170, the latter recruiting REST-corepressor complexes to promoters of Pax6 target genes involved in specification of IPs/LPs (and thus maintaining their expression in a repressed level) (Figure 7H). Loss of BAF170 in this early time window appears to lead to replacement of BAF170 by an additional BAF155 subunit, loss of the REST-corepressor complex and induction of euchromatin state that relieves the repression of Pax6 target genes involved in late neurogenesis. Thus, the biological outcome of BAF subunit exchange upon *BAF170*cKO is a heterochronic, premature expression of genes that specify IPs/LPs and facilitate indirect mode of neurogenesis. Conversely, overexpression of BAF170 during early neurogenesis and misexpression of BAF170 during late neurogenesis results in competition with BAF155 for occupancy of the BAF complex. This exerts effects on the chromatin status and expression of IP/LP genes in opposite manner to those of *BAF170*LOF condition, and thereby promoting the direct mode of neurogenesis.

DISCUSSION

Here, we investigate a potential role for mSWI/SNF complex for controlling generation of neurons in direct and indirect mode of cortical neurogenesis, ultimately affecting total cortical volume. We find that such a process indeed occurs and includes binding of the BAF170, BAF155, and Brm subunits of mSWI/SNF to TF Pax6, and recruitment of the REST-corepressor complex to promoters of *Pax6* downstream target genes involved in proliferation/specification of IPs and progenitors for late neurogenesis.

BAF170 Acts as a Modulator of Direct versus Indirect Neurogenesis

Present throughout the entire period of neurogenesis, the IPs shows a higher neurogenic fraction than does the apical RGCs (Pontious et al., 2008). Because of the limited proliferative capacity of IPs (Wu et al., 2005), control over the decision of RGCs to undergo direct or indirect neurogenesis via IPs has

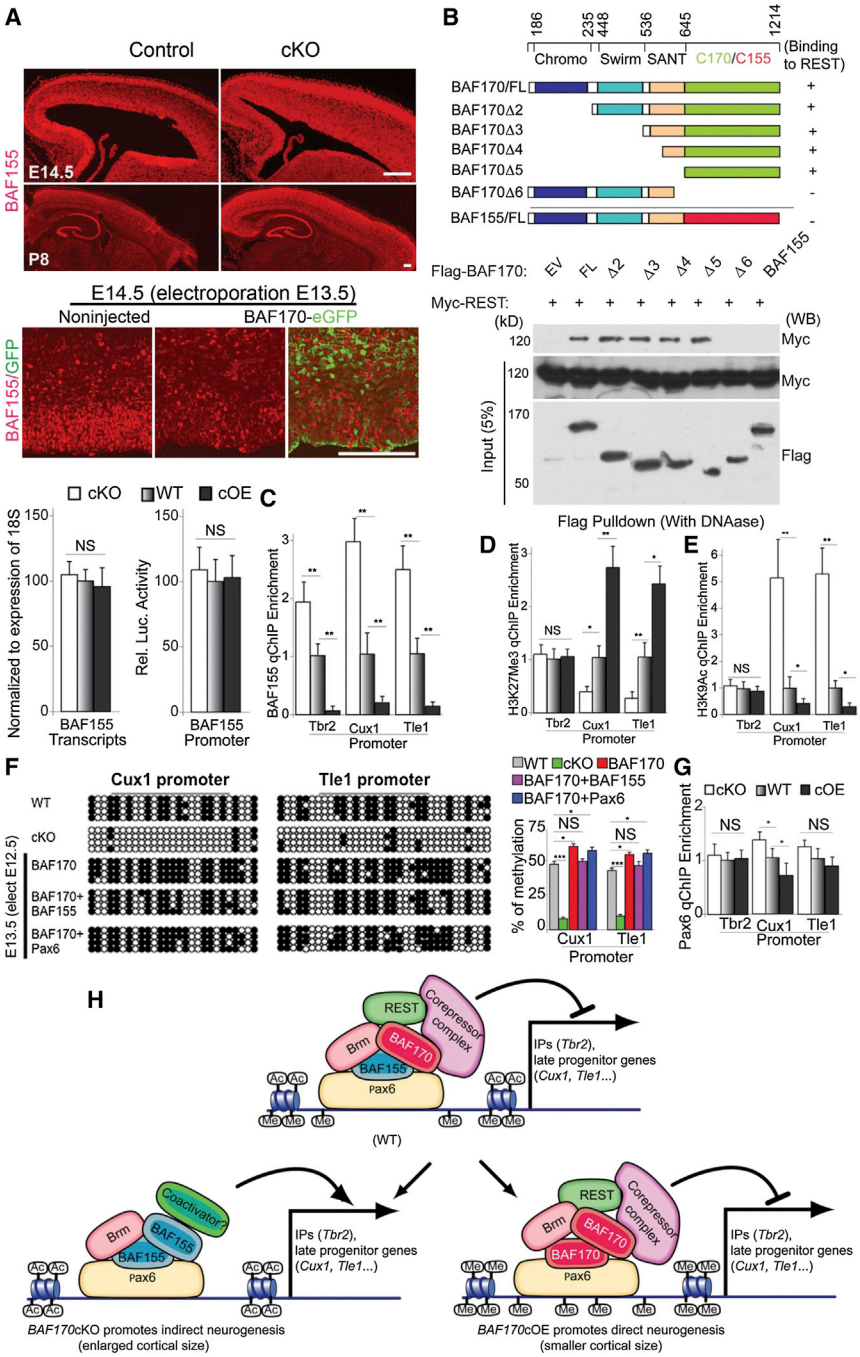

Figure 7. Change of *BAF170* Expression Level Causes a Subunit Alteration in the BAF Complex Affecting the Chromatin Structure and Binding of Pax6 and REST-Corepressor Complexes to Pax6 Target Genes

(A) Upper panel: IHC on sagittal E14.5 and P8 brain sections reveals enhanced BAF155 expression in *BAF170cKO* as compared to control cortex. Middle panel: focal overexpression of BAF170 via in utero electroporation of BAF170-ires-eGFP expression vector in E13.5 embryo brain results in abrogation of the BAF155 expression in VZ. Lowest panel: manipulation of BAF170 expression level in *cKO* and *cOE* mice affects neither the *BAF155* transcription nor *BAF155* promoter activity.

(B) The top scheme illustrates the structure of full-length (FL) BAF170 and BAF155, which consist of Chromo, Swirm, SANT, C-terminal of BAF170 (C170, in green), and C-terminal of BAF155 (C155, in red). To map BAF170/REST binding domains, a series of Flag-tagged BAF170 deletion constructs (Peng et al., 2009) were used in Flag pull-down assays employing lysates of HeLa cells transfected with a Myc-REST expression construct. The top blot shows eluted proteins after immunoprecipitation with Flag antibody; the bottom blots show the input proteins. Note that BAF170 fragment without C170 domain (BAF170Δ6) and full-length BAF155 lack binding capacity to REST.

(C–E and G) ChIP analyses for *Tbr2*, *Cux1*, *Tle1* promoter occupancy by BAF155 (C), repressive marks H3K27Me3 (D), active chromatin marks H3K9Ac (E), and Pax6 (G) in NSC derived from *BAF170*cKO, control, and *BAF170*cOE cortices. In (C) loss or overexpression of *BAF170* causes opposite change, enrichment or abolishment of BAF155 on the assayed promoters. (D and E) Similarly, loss of *BAF170* (*BAF170*cKO cortex) increases the activation-associated chromatin modification on *Cux1* and *Tle1* promoters, which both become repressed in *BAF170*cOE cortex. (G) Loss and overexpression of BAF170 significantly enhances and diminishes Pax6 binding to *Cux1* promoter, respectively and tended to have similar effects on the *Tle1* promoter.

(F) Bisulfite sequencing analysis of CpG methylation on *Cux1* and *Tle1* promoters using genomic DNA isolated from control and *BAF170*cKO cortices, or cortices electroporated at E12.5 with the indicated expression plasmids: BAF170, mixture BAF170/BAF155 (1:1), BAF170/Pax6 (1:1). Note the substantial decrease of CpG methylation (repressive marks) in *BAF170*cKO cortex, and the increase upon BAF170 overexpression. This phenotype is partially rescued upon cotransfection with both *BAF170* and *BAF155* expression plasmids, but not with a mixture of *BAF170* and *Pax6* plasmids. The bottom left diagram (in colors) presents the statistical analyses for methylation frequency within *Cux1* and *Tle1* promoters.

(H) Hypothetical model proposing how a subunit exchange in mSWI/SNF in *BAF170*cKO and *BAF170*cOE cortices, and coupling between TFPax6, BAF170, BAF155, and REST-corepressor complex controls expression of genes involved in IP/LP genesis. Statistical analyses were done using Student's t test. Values are presented as means ± SEM (n = 4). Scale bars represent 250 μm.

See also Figure S7.

important implications for the timing of neurogenesis, total neuronal output and cortical morphogenesis.

Changes in the subunit composition of the mSWI/SNF chromatin-remodeling complexes esBAF, npBAF, and nBAF parallel the acquisition of either neural progenitor (npBAF) or mature neuronal (nBAF) fates from embryonic stem cells (esBAF) (Ho et al., 2009; Yoo and Crabtree, 2009). BAF170 is a specific component of the npBAF complex. Here, we show that in the

developing cortex the presence of BAF170 in the mSWI/SNF exerts control over IPs generation. Deficiency of BAF170 expression in the *BAF170cKO* mice resulted in a transient decrease in early-born neuronal subsets, inhibition of progenitor cell-cycle exit and generation of a surplus of Tbr2$^+$ IPs. Because the RGC pool appeared unaltered in the *BAF170*cKO mice, these findings collectively indicate that when *BAF170* is absent at the onset of neurogenesis, the RGPs generate less than the normal number of LL neurons (e.g., the Tuj1$^+$, Ctip2$^+$, and ER81$^+$ subsets) by direct neurogenesis, and instead produce many more IPs. At later stages, IPs rebuild the LL neuronal pool, generating a modest surplus of LL neuronal sublineages (FoxP2$^+$ L6, Tle4$^+$ L5a, Ctip2$^+$ L5b$^+$, ER81$^+$ L5$^+$) at normal and ectopic positions in the postnatal *BAF170*cKO cortex, as well as a large excess of neurons with UL fates. The opposite phenotype was observed upon BAF170 overexpression in cortical progenitors in the *BAF170*cOE mice, including the promotion of direct neurogenesis, depletion of the Tbr2$^+$ IP pool, and diminished cortical size. The observed defects in *BAF170*cOE mice are very similar to those in *Tbr2* LOF mutants (Sessa et al., 2008), which also show a severe loss of IPs, and enhanced early neurogenesis coupled to a reduction in the total neuronal output at maturity. Importantly, in the rescue experiment, the cortex of the double *BAF170*cKO/*Pax6*cKO mice (dcKO) showed a similar number of Tbr2$^+$ IPs compared to that in control, indicating that a genetic interaction between Pax6 and BAF170 governs the expression of *Tbr2* and the genesis of IPs.

Taken together, these findings indicate that BAF170 plays an essential role in modulating direct and indirect cortical neuronal output, thereby influencing the composition of LL and UL laminae, thus controlling the cortical size and thickness.

BAF170 and the Stoichiometric Composition of the SWI/SNF Complex in Cortical Neurogenesis

mSWI/SNF complex contains a core catalytic ATPase subunit (Brg1 or Brm) and more than 10 associated BAF factors (Wang et al., 1996). To maintain a correct stoichiometric protein level in the cell, the expression and degradation of the multiple SWI/SNF subunits are strictly controlled. We showed here that loss of BAF170 expression in the nonneurogenic RGCs led to elevation of BAF155 protein levels, thus altering mSWI/SNF composition. It has been shown that addition of BAF155 (alone or together with Brg1) enhances the reprogramming mediated by Oct4, Sox2, Klf4, and Myc in ES cells, suggesting that incorporation of BAF155 promotes a euchromatic chromatin state in the promoters of these genes, endowing a pluripotency (Singhal et al., 2010). Together, these findings suggest that upon *BAF170*LOF and GOF, changes in the balance between BAF170 and BAF155-containing SWI/SNF complexes in cortical RGCs result in chromatin rearrangement on the genomic loci of Pax6 target genes. Furthermore, the results suggest that at E12.5–E14.5 (when BAF170 expression is confined to mitotically active apical RGPs), the correct switch from direct to indirect mode of neurogenesis depends on the relative amounts of BAF170 and BAF155 in the mSWI/SNF complex. In support of such scenario, our preliminary data indicate that the loss of BAF155 in *BAF155cKO* mice severely affects the generation of IPs and cortical layering in a manner, opposite to those of the *BAF170cKO* mice (T.C.T. and A.S., unpublished data).

During development, a diversity of BAF complexes controls distinct transcriptional programs (Wang et al., 1996; Lessard et al., 2007; Ho et al., 2009). According to a current model, mSWI/SNF complexes with the core catalytic ATPase subunits Brg/Brm are necessary for changing the nucleosomal structure of targeted genomic loci (Wu et al., 2009; Yoo and Crabtree, 2009). To generate specificity, distinct BAF subunits interact with specific transcription factors, recruiting the complex to the sites of action of the corresponding factors. TF Pax6 is a multifunctional, controlling both NSC self-renewal and neuronal differentiation in a highly context- and dose-dependent fashion (Sansom et al., 2009). We found that during early neurogenesis, BAF170 and BAF155 together with Brm bind to Pax6, exerting indirect repressive control by recruiting REST-corepressor complex to the promoters of at least three Pax6 downstream target genes (*Tbr2*, *Cux1*, and *Tle1*) involved in generation of neurons via IP. Furthermore, we showed that Pax6 specifically recruits Brm, but not Brg1, to the promoters of the three Pax6 target genes, indicating that BAF170 and Brm act in the same BAF complex during early neurogenesis. In another context however, such as during lens differentiation, Pax6 is known to directly recruit the Brg1 ATPase as a core subunit to the *crystallin* gene locus (Yang et al., 2006).

Interaction of Pax6 with the mSWI/SNF Chromatin Remodeling Complex Mediates Epigenetic Control of Target Gene Expression

Given that the REST-corepressor complex binds specifically to BAF170 (Battaglioli et al., 2002), the replacement of BAF170 with BAF155 in the *BAF170*cKO mouse cortex leads to two consequences for Pax6-dependent transcriptional control: (1) elimination of the REST-corepressor complex from the promoters of the three studied Pax6-downstream target genes, and (2) induction of euchromatin state, thus enhancing heterochronically the accessibility of Pax6 to these target promoters. Because BAF57 interacts with the REST-corepressor complex (including REST, CoREST, MeCP2, HDACs) that mediates transcriptional repression (Battaglioli et al., 2002; Harikrishnan et al., 2005), the detected lower level of BAF57 in BAF170LOF might also contribute to this phenotype.

Although both Pax6 and BAF170 directly bind to the promoters of *Tbr2*, *Cux1*, and *Tle1*, the expression of these IP or LP marker genes appears to be controlled by different mechanisms. In the case of *Cux1* and *Tle1*, we found that alteration of the expression of *BAF170* caused a BAF155-dependent change in chromatin structure, assessed by the altered expression of repressive (H3K9Ac) or active (H3K9Ac) marks. The results strongly suggest that during early neurogenesis, epigenetic chromatin regulation by BAF170 inhibits the expression of these two late progenitor genes (*Cux1* and *Tle1)*. In contrast, neither *BAF170*LOF nor *BAF170*GOF affects epigenetic marks on the nonmethylated *Tbr2* promoter. Given that *Tbr2* expression is regulated by multiple TFs, including Pax6 and its target genes *Ngn2* and *AP2*γ (Ochiai et al., 2009; Pinto et al., 2009), it appears that Pax6-dependent transcriptional, rather than epigenetic control is essential for activating *Tbr2*. In the same line of evidence, in contrast with the almost fully rescued Tbr2$^+$ IP-related phenotype, the cortex of the double *BAF170cKO/Pax6*cKO mutants still showed a greater number of Cux1$^+$ UL neurons than that

of control. These data implicate that BAF170 may control the production of distinct upper layer neuronal subsets (including the Cux1$^+$ upper layer neurons) via additional mechanisms, rather than only through interactions with Pax6.

The IPs, present in the VZ/SVZ throughout the entire neurogenic period, are generated by asymmetric divisions of RGCs, and act as amplifiers of neuronal fates. Accordingly, regulation of the IP pool size has an important impact on cortical morphogenesis both during development and evolution. As a part of complex molecular interactions influenced by chromatin remodeling, we showed here that BAF170 mediates the interaction between Pax6 and the REST corepressor complex on promoters of a set of Pax6 targets, involved in the RGCs decision for direct-versus-indirect neurogenesis. Our findings reveal a epigenetic mechanism for controlling the modes of neurogenesis in developing mammalian cortex, defining the cortical size, thickness and cellular composition of the cortex in the adult brain.

EXPERIMENTAL PROCEDURES

Animals

A list of mouse strains with detailed descriptions is provided in the Supplemental Experimental Procedures. Animals were handled in accordance with the German Animal Protection Law and with the permission of the Bezirksregierung Braunschweig.

Plasmids and Antibodies

A list of plasmids and antibodies with detailed descriptions is provided in Supplemental Information.

Protein-Protein Interaction Assay

Flag IP were performed as described previously (Tuoc and Stoykova, 2008b). A detailed procedure for in vivo IP with anti-BAF170, anti-Pax6 antibodies and Flag IP is provided in the Supplemental Experimental Procedures.

mRNA Expression Profiling and Data Analysis

RNA was extracted (RNAeasy kit, QIAGEN) from both cortices from three control and three *BAF170*cKO E12.5 littermate mice. Gene expression in each sample was assayed using Illumina Mouse WG6 v2.0 BeadChip microarrays (Cambridge Genomic Services). Genes showing significant changes in expression in the *BAF170*cKO were compared with genes previously identified as Pax6-regulated in the *D6-Pax6* and/or *Sey/Sey* E12.5 neocortex (Sansom et al., 2009). Detailed descriptions of data analysis are provided in the Supplemental Experimental Procedures.

EMSA, ChIP, Bisulfite Genomic Analysis, and qRT-PCR

EMSA, ChIP, bisulfite genomic analysis, and qRT-PCR methods have been described previously (Tuoc and Stoykova, 2008b). A detailed procedure, including some modifications, is provided in the Supplemental Experimental Procedures.

Cortical Progenitor Culture and Reporter Assay

Detailed descriptions are provided in the Supplemental Experimental Procedures.

IHC and Cell-Cycle Index

After blocking with 5% goat or donkey normal sera sections were incubated overnight with primary antibody at 4°C, and the signal was detected with a fluorescent secondary antibody (Alexa Fluor; 1:400; Invitrogen). Cell cycle exit was determined on coronal sections of E14.5 brains 24 hr after BrdU injection (140 μg/g) of pregnant mice at E13.5. After double IHC with BrdU and Ki67 antibodies, the cell-cycle index was calculated as the number of BrdU$^+$/Ki67-cells divided by total BrdU$^+$cells.

Relative Quantification of Cortical Size

Dorsal views of forebrains of mutant and control mice at P8–P10 were photographed under a dissection microscope. Cortical anterior-posterior axis (AP), cortical surface and midline lengths from the digitized images were processed to compare above parameters between mutants and controls by using NIH ImageJ software (Sahara and O'Leary, 2009).

In Vivo MRI

MRI was performed on 5 *BAF170*cKO and 5 *BAF170*cOE mice and their respective controls (n = 5/5) at the age of 11 and 6 weeks, respectively. Mice were anesthetized with 5% isoflurane, intubated and kept under anesthesia with 1.75% isoflurane in ambient air. For a proper separation between gray and white matter magnetization transfer (MT) weighted 3D MRI were obtained at 9.4 T (Bruker Biospin) with 100 μm isotropic spatial resolution (FLASH, TR/TE = 14.9/3.9 ms, flip angle: 5°, MT-weighting: Gaussian-shaped off-resonance irradiation, frequency offset: 3 kHz, pulse duration: 3.5 ms, flip angle: 135°). Brain height and mean cortical thickness were assessed on 2 parasagittal sections (~0.3 mm left and right to the midline). Cortical volume and surface area were determined by manual segmentation of the neocortex using the software package Amira 4.1.1 (Boretius et al., 2009).

Image Analysis and Cell Counts

Images were captured with an Olympus BX60 microscope or a laser confocal microspore (Leica TCS Sp5) and processed with Adobe Photoshop (Version CS2).

Anatomically matched coronal brain sections of the rostral cortex at the level of septum (100–300 μm caudally of the appearance of the anterior commissure) were used. Counting of immunostained cells was performed in equally sized digitalized frames in the presumptive fields of the primary somatosensory or motor area, as indicated in legends for Figures 3 and 4. Quantification on sagittal brains sections at postnatal (P) stages P10 and P8 was done in the somatosensory area at a level ~300–800 μm apart the midline. Because cortical phenotypes revealed by the in vivo MRI stereological analysis showed consistent penetration, in most cases the cell counts of four sections were averaged from two biological replicate (control/mutant brain pairs).

Statistical Analysis

All statistical analyses were done using Student's t test, except the data in Figure 2 (with Mann-Whitney test) and the data in Figure 5B (with hypergeometric test). All graphs are plotted as mean ± SEM.

ACCESSION NUMBERS

The NCBI's Gene Expression Omnibus accession number for the microarray data reported in this article is GSE45629.

SUPPLEMENTAL INFORMATION

Supplemental Information includes seven figures, one table, and Supplemental Experimental Procedures and can be found with this article online at http://dx.doi.org/10.1016/j.devcel.2013.04.005.

ACKNOWLEDGMENTS

We acknowledge L. Pham, S. Schlott, and M. Daniel for their excellent technical assistance and H. Fett, U. Franke, and S. Mahsur for the generation and care of transgenic mice. We thank M. Kessel for his support and G. Crabtree, R. H. Seong, F. Guillemot, T. Miyata, S. Arber, D. Anderson, K. Nave, A. Messing, K. Jones, H.F. Jorgensen, and S.Y. Lin for providing reagents or mouse lines. This work was supported by the Max Planck Gesellschaft and the Cluster of Excellence "Nanoscale Microscopy and Molecular Physiology of the Brain (CNMPB)," Göttingen. A.S. and T.C.T. conceived and wrote the manuscript. T.C.T. designed and carried most experiments. S.B. and J.F. performed MRI measurement. S.N.S. and F.J.L. contributed in analyses of *Pax6/BAF170* transcriptome comparison and discussion of the manuscript. M.-E.P. carried out BAF170 co-IP in vivo.

Received: August 8, 2012
Revised: February 21, 2013
Accepted: April 7, 2013
Published: May 2, 2013

REFERENCES

Ballas, N., Grunseich, C., Lu, D.D., Speh, J.C., and Mandel, G. (2005). REST and its corepressors mediate plasticity of neuronal gene chromatin throughout neurogenesis. Cell *121*, 645–657.

Battaglioli, E., Andres, M.E., Rose, D.W., Chenoweth, J.G., Rosenfeld, M.G., Anderson, M.E., and Mandel, G. (2002). REST repression of neuronal genes requires components of the hSWI.SNF complex. J Biol Chem *277*, 41038–41045.

Bertrand, N., Castro, D.S., and Guillemot, F. (2002). Proneural genes and the specification of neural cell types. Nat. Rev. Neurosci. *3*, 517–530.

Boretius, S., Michaelis, T., Tammer, R., Ashery-Padan, R., Frahm, J., and Stoykova, A. (2009). In vivo MRI of altered brain anatomy and fiber connectivity in adult pax6 deficient mice. Cereb. Cortex *19*, 2838–2847.

Buscarlet, M., Perin, A., Laing, A., Brickman, J.M., and Stifani, S. (2008). Inhibition of cortical neuron differentiation by Groucho/TLE1 requires interaction with WRPW, but not Eh1, repressor peptides. J Biol Chem *283*, 24881–24888.

Chen, Z.F., Paquette, A.J., and Anderson, D.J. (1998). NRSF/REST is required in vivo for repression of multiple neuronal target genes during embryogenesis. Nat. Genet. *20*, 136–142.

Cubelos, B., Sebastián-Serrano, A., Kim, S., Redondo, J.M., Walsh, C., and Nieto, M. (2008). Cux-1 and Cux-2 control the development of Reelin expressing cortical interneurons. Dev. Neurobiol. *68*, 917–925.

Fuentes, P., Cánovas, J., Berndt, F.A., Noctor, S.C., and Kukuljan, M. (2012). CoREST/LSD1 control the development of pyramidal cortical neurons. Cereb. Cortex *22*, 1431–1441.

Gajović, S., St-Onge, L., Yokota, Y., and Gruss, P. (1997). Retinoic acid mediates Pax6 expression during in vitro differentiation of embryonic stem cells. Differentiation *62*, 187–192.

Georgala, P.A., Manuel, M., and Price, D.J. (2011). The generation of superficial cortical layers is regulated by levels of the transcription factor Pax6. Cereb. Cortex *21*, 81–94.

Goebbels, S., Bormuth, I., Bode, U., Hermanson, O., Schwab, M.H., and Nave, K.A. (2006). Genetic targeting of principal neurons in neocortex and hippocampus of NEX-Cre mice. Genesis *44*, 611–621.

Götz, M., and Huttner, W.B. (2005). The cell biology of neurogenesis. Nat. Rev. Mol. Cell Biol. *6*, 777–788.

Götz, M., Stoykova, A., and Gruss, P. (1998). Pax6 controls radial glia differentiation in the cerebral cortex. Neuron *21*, 1031–1044.

Harikrishnan, K.N., Chow, M.Z., Baker, E.K., Pal, S., Bassal, S., Brasacchio, D., Wang, L., Craig, J.M., Jones, P.L., Sif, S., et al. (2005). Brahma links the SWI/SNF chromatin-remodeling complex with MeCP2-dependent transcriptional silencing. Nat Genet *37*, 254–264.

Hevner, R.F., Hodge, R.D., Daza, R.A., and Englund, C. (2006). Transcription factors in glutamatergic neurogenesis: conserved programs in neocortex, cerebellum, and adult hippocampus. Neurosci. Res. *55*, 223–233.

Ho, L., Ronan, J.L., Wu, J., Staahl, B.T., Chen, L., Kuo, A., Lessard, J., Nesvizhskii, A.I., Ranish, J., and Crabtree, G.R. (2009). An embryonic stem cell chromatin remodeling complex, esBAF, is essential for embryonic stem cell self-renewal and pluripotency. Proc. Natl. Acad. Sci. USA *106*, 5181–5186.

Kriegstein, A., Noctor, S., and Martínez-Cerdeño, V. (2006). Patterns of neural stem and progenitor cell division may underlie evolutionary cortical expansion. Nat. Rev. Neurosci. *7*, 883–890.

Lessard, J., Wu, J.I., Ranish, J.A., Wan, M., Winslow, M.M., Staahl, B.T., Wu, H., Aebersold, R., Graef, I.A., and Crabtree, G.R. (2007). An essential switch in subunit composition of a chromatin remodeling complex during neural development. Neuron *55*, 201–215.

Lunyak, V.V., Burgess, R., Prefontaine, G.G., Nelson, C., Sze, S.H., Chenoweth, J., Schwartz, P., Pevzner, P.A., Glass, C., Mandel, G., and Rosenfeld, M.G. (2002). Corepressor-dependent silencing of chromosomal regions encoding neuronal genes. Science *298*, 1747–1752.

Molyneaux, B.J., Arlotta, P., Menezes, J.R., and Macklis, J.D. (2007). Neuronal subtype specification in the cerebral cortex. Nat. Rev. Neurosci. *8*, 427–437.

Ochiai, W., Nakatani, S., Takahara, T., Kainuma, M., Masaoka, M., Minobe, S., Namihira, M., Nakashima, K., Sakakibara, A., Ogawa, M., and Miyata, T. (2009). Periventricular notch activation and asymmetric Ngn2 and Tbr2 expression in pair-generated neocortical daughter cells. Mol. Cell. Neurosci. *40*, 225–233.

Peng, G., Yim, E.K., Dai, H., Jackson, A.P., Burgt, I., Pan, M.R., Hu, R., Li, K., and Lin, S.Y. (2009). BRIT1/MCPH1 links chromatin remodelling to DNA damage response. Nat Cell Biol *11*, 865–872.

Pinto, L., Mader, M.T., Irmler, M., Gentilini, M., Santoni, F., Drechsel, D., Blum, R., Stahl, R., Bulfone, A., Malatesta, P., et al. (2008). Prospective isolation of functionally distinct radial glial subtypes—lineage and transcriptome analysis. Mol. Cell. Neurosci. *38*, 15–42.

Pinto, L., Drechsel, D., Schmid, M.T., Ninkovic, J., Irmler, M., Brill, M.S., Restani, L., Gianfranceschi, L., Cerri, C., Weber, S.N., et al. (2009). AP2gamma regulates basal progenitor fate in a region- and layer-specific manner in the developing cortex. Nat. Neurosci. *12*, 1229–1237.

Pontious, A., Kowalczyk, T., Englund, C., and Hevner, R.F. (2008). Role of intermediate progenitor cells in cerebral cortex development. Dev. Neurosci. *30*, 24–32.

Quinn, J.C., Molinek, M., Martynoga, B.S., Zaki, P.A., Faedo, A., Bulfone, A., Hevner, R.F., West, J.D., and Price, D.J. (2007). Pax6 controls cerebral cortical cell number by regulating exit from the cell cycle and specifies cortical cell identity by a cell autonomous mechanism. Dev Biol *302*, 50–65.

Sansom, S.N., Griffiths, D.S., Faedo, A., Kleinjan, D.J., Ruan, Y., Smith, J., van Heyningen, V., Rubenstein, J.L., and Livesey, F.J. (2009). The level of the transcription factor Pax6 is essential for controlling the balance between neural stem cell self-renewal and neurogenesis. PLoS Genet. *5*, e1000511.

Sahara, S., and O'Leary, D.D. (2009). Fgf10 regulates transition period of cortical stem cell differentiation to radial glia controlling generation of neurons and basal progenitors. Neuron *63*, 48–62.

Sessa, A., Mao, C.A., Hadjantonakis, A.K., Klein, W.H., and Broccoli, V. (2008). Tbr2 directs conversion of radial glia into basal precursors and guides neuronal amplification by indirect neurogenesis in the developing neocortex. Neuron *60*, 56–69.

Singhal, N., Graumann, J., Wu, G., Araúzo-Bravo, M.J., Han, D.W., Greber, B., Gentile, L., Mann, M., and Schöler, H.R. (2010). Chromatin-Remodeling Components of the BAF Complex Facilitate Reprogramming. Cell *141*, 943–955.

Tuoc, T.C., and Stoykova, A. (2008a). Er81 is a downstream target of Pax6 in cortical progenitors. BMC Dev. Biol. *8*, 23.

Tuoc, T.C., and Stoykova, A. (2008b). Trim11 modulates the function of neurogenic transcription factor Pax6 through ubiquitin-proteosome system. Genes Dev. *22*, 1972–1986.

Tuoc, T.C., Radyushkin, K., Tonchev, A.B., Piñon, M.C., Ashery-Padan, R., Molnár, Z., Davidoff, M.S., and Stoykova, A. (2009). Selective cortical layering abnormalities and behavioral deficits in cortex-specific Pax6 knock-out mice. J. Neurosci. *29*, 8335–8349.

Wang, W., Xue, Y., Zhou, S., Kuo, A., Cairns, B.R., and Crabtree, G.R. (1996). Diversity and specialization of mammalian SWI/SNF complexes. Genes Dev. *10*, 2117–2130.

Weissman, T., Noctor, S.C., Clinton, B.K., Honig, L.S., and Kriegstein, A.R. (2003). Neurogenic radial glial cells in reptile, rodent and human: from mitosis to migration. Cereb. Cortex *13*, 550–559.

Wu, S.X., Goebbels, S., Nakamura, K., Nakamura, K., Kometani, K., Minato, N., Kaneko, T., Nave, K.A., and Tamamaki, N. (2005). Pyramidal neurons of upper cortical layers generated by NEX-positive progenitor cells in the subventricular zone. Proc. Natl. Acad. Sci. USA *102*, 17172–17177.

Wu, J.I., Lessard, J., and Crabtree, G.R. (2009). Understanding the words of chromatin regulation. Cell *136*, 200–206.

Yan, Z., Wang, Z., Sharova, L., Sharov, A.A., Ling, C., Piao, Y., Aiba, K., Matoba, R., Wang, W., and Ko, M.S. (2008). BAF250B-associated SWI/SNF chromatin-remodeling complex is required to maintain undifferentiated mouse embryonic stem cells. Stem Cells *26*, 1155–1165.

Yang, Y., Stopka, T., Golestaneh, N., Wang, Y., Wu, K., Li, A., Chauhan, B.K., Gao, C.Y., Cveklová, K., Duncan, M.K., et al. (2006). Regulation of alphaA-crystallin via Pax6, c-Maf, CREB and a broad domain of lens-specific chromatin. EMBO J. *25*, 2107–2118.

Yoo, A.S., and Crabtree, G.R. (2009). ATP-dependent chromatin remodeling in neural development. Curr. Opin. Neurobiol. *19*, 120–126.

Zhuo, L., Theis, M., Alvarez-Maya, I., Brenner, M., Willecke, K., and Messing, A. (2001). hGFAP-cre transgenic mice for manipulation of glial and neuronal function in vivo. Genesis *31*, 85–94.